Analysis of OPLL type according to classification A and axial classification in 144 patients

Classification A

Fifty-four patients (37.5 %) had a bridge formation between vertebral bodies on the sagittal plane. Bridge formation occurred from vertebral bodies 2–8: in 28 patients at two levels, four patients at three levels, five patients at four levels, and 17 patients at more than five levels (Table 1). Twelve patients had bridge formation in two separate areas, shown as 2 + 2 (2-level bridge + 2-level bridge), 2 + 3, 4 + 4 and 2 + 5 (Table 1 and Fig. 2). Ninety patients had nonbridge OPLL.

Axial classification

One hundred and two patients (70.8 %) had central-type OPLL, and 42 (29.2 %) had the lateral type.

Case presentation

Case 1

The patient, a 59-year-old man, had mixed type OPLL according to X-ray of the cervical spine (Fig. 3a). He had the bridge type according to classification A, as OPLL was seen from C5–7 and was connected to vertebral bodies (Fig. 3b). In classification B, the OPLL lesion was expressed as "C③/4, 5–7". The spinal canal was the narrowest at C4. Ossification was classified as the central type on axial image at C4 (Fig. 3c).

Case 2

A 74-year-old had a C3–7 laminoplasty 5 years earlier. His OPLL was classified as continuous based on cervical X-ray (Fig. 4a). According to classification A, he had bridge type OPLL from C3 to T2 (Fig. 4b). OPLL lesions were expressed as "C3–7" according to classification B and left lateral type at C5–6 according to axial classification (Fig. 4c).

Case 3

A 69-year-old woman with OPLL considered as the segmental type according to X-ray (Fig. 5a). She had the nonbridge type at C4 and C5 and was classified as "C4.5.6" according to classification B (Fig. 5b). She had the central type in axial classification at C5, where the OPLL was the most pronounced (Fig. 5c).

Case 4

A 66-year-old man had mixed OPLL according to cervical X-ray (Fig. 6a), bridge type in classification A, expressed as "C②/3–4/5/6" in classification B (Fig. 6b) and as central type in axial classification at C3 level (Fig. 6c).

Discussion

Lateral X-ray examination is the gold standard by which to determine the existence of OPLL in the cervical spine and by which most physicians establish the diagnosis. OPLL classification by lateral X-ray, proposed by the Investigation Committee on OPLL of the Japanese Ministry of Public Health and Welfare in 1981, has widely been used

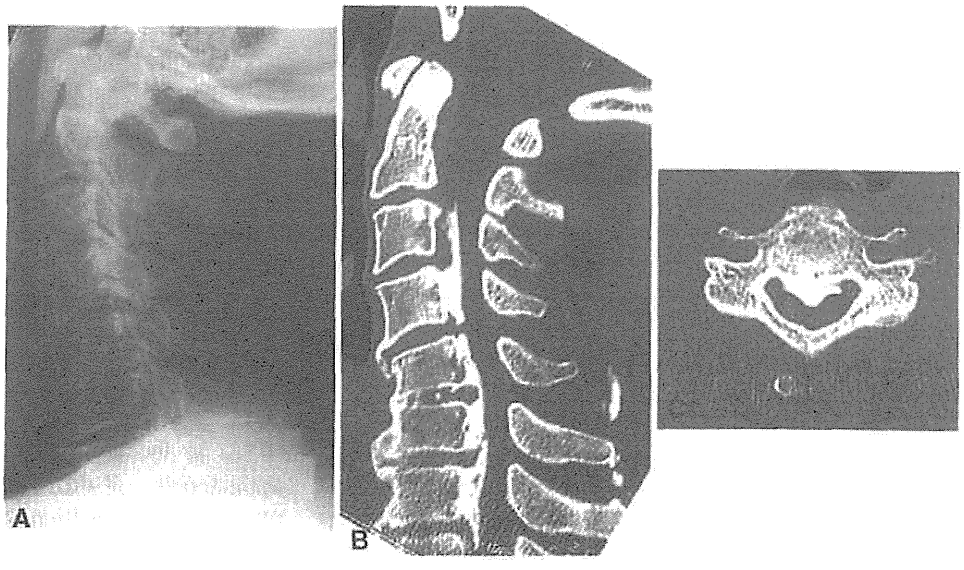

Fig. 3 A 59-year-old man. Lateral cervical X-ray (a), midsagittal computed tomography (CT) image (b), and axial CT image at C4 (c)

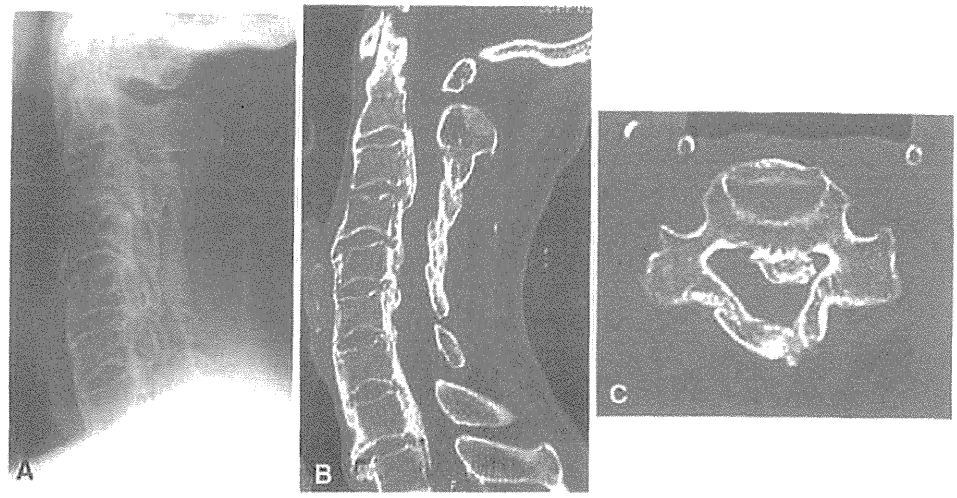

Fig. 4 A 74-year-old man. Lateral cervical X-ray (a), midsagittal computed tomography (CT) image (b), and axial CT image at C5–6 level (c)

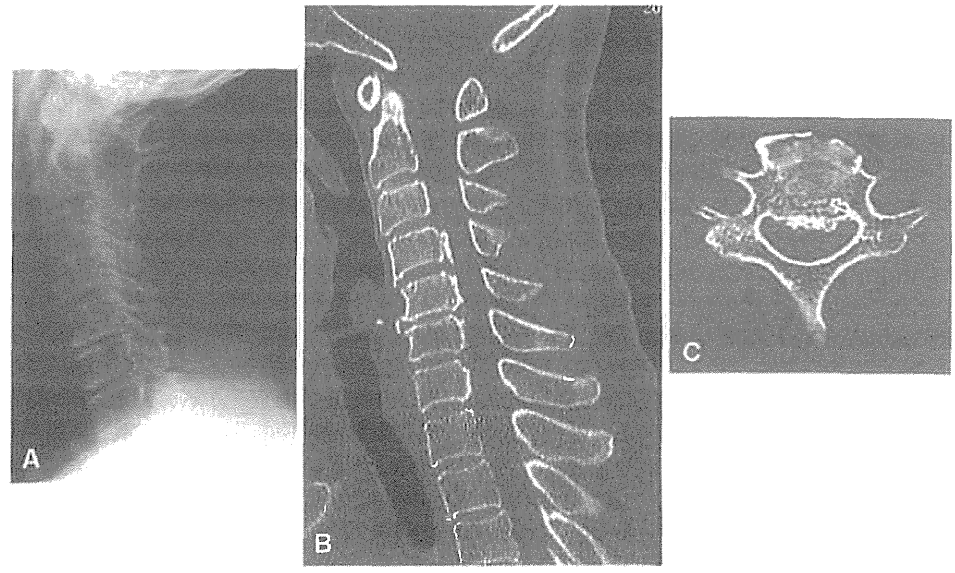

Fig. 5 A 69-year-old woman. Lateral cervical X-ray (a), midsagittal computed tomography (CT) (b), and axial CT at C5 level (c)

[6] and is useful for assessing OPLL characteristics because it is easy to identify ossified lesions and is beneficial for predicting OPLL progression and the occurrence of cervical myelopathy. However, the lateral X-ray does not provide details of lesions themselves. A recent study has shown that CT imaging is necessary for precise detection of such lesions [9]. In fact, CT has become a standard tool for evaluating such ossified lesions, and most spine surgeons obtain CT imaging before surgical intervention in patients with OPLL. Therefore, we decided to develop a new classification system of OPLL based on CT imaging.

In classification A, we noted bridge formation of ossified lesions to the vertebral body for the following two reasons: (1) The absence of bridge formation is directly related to segmental motion of vertebrae, which is lost at the level where the bridge is formed [10]. On the other hand, the segment adjacent to the bridge formation might have greater motion, which results in adjacent segmental instability. It has been reported that segmental motion is a factor causing neurological impairment, such as cervical myelopathy [11]. In their long-term follow-up study, Matsunaga et al. [11] stated that range of motion (ROM) was significantly larger in patients with than those without myelopathy. They emphasized the importance of cervical motion that might lead to the development of neurological compromise. (2) Bridge formation may be related to the extension of ossified lesions along the entire spine. Matsunaga et al. also demonstrated that bridge formation in OPLL in the cervical spine is strongly related to multiple OPLL in the entire spine [9] and might represent the characteristics of diffuse ossification in PLL in the entire spine. Bridge formation can be precisely evaluated by CT imaging, but it is difficult to assess the finding using lateral

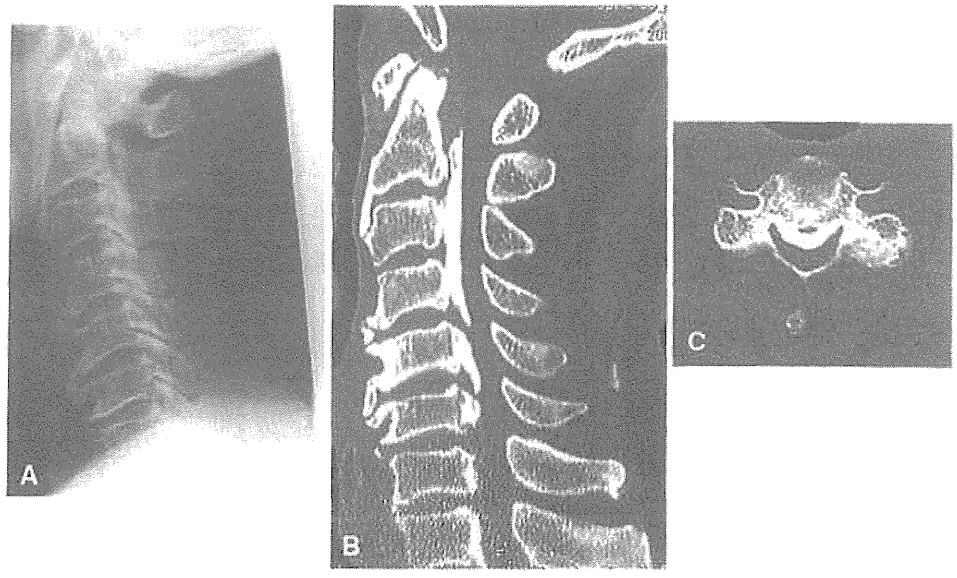

Fig. 6 A 66-year-old man. Lateral cervical X-ray (a), midsagittal computed tomography (CT) image (b), and axial CT image at C3 (c)

X-ray alone. In classification A, the interrater agreement ratio was 0.43 among the seven examiners, indicating moderate agreement. Interrater agreement ratio was not high but seems to be acceptable according to evaluation among the seven examiners. This low ratio might be due to examiners' unfamiliarity with evaluating ossified lesions on CT images. In particular, it is difficult to judge the bony bridge on a CT image if the small ossification connects to the adjacent vertebrae. It might be important to check segmental motion in order to evaluate connection or disconnection between adjacent vertebrae. When the examiners become familiar with the evaluation technique using CT images, the agreement ratio might increase. The averaged intrarater reliability was 72.4 %, which indicates substantial agreement. Therefore, we believe that this classification system is very easy to use and has the potential benefit for evaluating characteristics of cervical OPLL lesions.

CT provides an excellent axial view of the spinal canal, yielding valuable information on the area and median or paramedian location of ossification. In axial-image classification, we selected the level where OPLL most frequently occurs in the spinal canal. Information regarding the ratio of ossified lesions to the spinal canal is very important, because previous report indicate that patients with ≥60 % of the cervical spinal canal/stenosis by OPLL had cervical myelopathy [12, 13]. Laterality of the ossified lesion can be evaluated using this classification. Patients with cervical myelopathy due to OPLL sometimes have a predominant side of neurological impairment [12]. However, data of patients' clinical symptoms were not included in the study reported here. The relationship between the axial classification and clinical symptoms will be an important research theme for future studies.

For classification B, we evaluated ossified lesions at all vertebral and intervertebral levels and checked for and described their connection or disconnection and whether or not lesions are attached to the upper or lower border of the vertebral body. This classification provides a precise means of identifying the existence of OPLL lesions and, if they are present, describes their characteristics. However, this classification is somewhat complex, and we believe it may not be appropriate for daily clinical use but, rather, may be useful for precise data collection in future studies.

This study has several limitations. First, we did not check the dynamic factor or cervical spine alignment using CT images. CT was taken with the patient in a supine position without performing flexion and extension analysis. Thus, segmental motion could not be detected. Second, we did not evaluate the relationship between OPLL types and clinical symptoms. In the axial image, the occupied ratio against the spinal canal can be easily detected. It might be interesting to determine how laterality is related to the predominant side of the neurological deficit; however, we have no MRI information regarding spinal cord compression due to OPLL. The relationship of OPLL lesions and/or dynamic factors to clinical symptoms is a theme for future study. Thirdl, the agreement ratio for both types of classification A is moderate, although we consider it acceptable for use. Classification B is a highly complicated procedure, and we thus did not analyze intra- or interobserver agreement ratio. Despite these several study limitations, CT classification provides precise evaluation of OPLL lesions and might also be useful to help determine the appropriate operative procedure. For example, fusion surgery is not necessary at a level where there is bridge formation, because there is no segment motion at that level. This might be the advantage of CT classification over X-ray classification.

In conclusion, we, the subcommittee members of the Investigation Committee on the Ossification of the Spinal Ligaments of the Japanese Ministry of Public Health and Welfare, propose three new classification systems for cervical OPLL based on CT imaging: classification A, classification B, and the axial image classification. It is our hope that these classifications will be recognized as useful clinical assessment tools for evaluating OPLL lesions.

Acknowledgments This work was supported by Health Labour Sciences Research Grant, Research on intractable diseases, Committee for Study of Ossification of Spinal Ligament. The authors thank Mika Kigawa, assistant professor, Department of Public Health, Toyama University, for statistical assistance.

Conflict of interest The authors declare that they have no conflict of interest.

References

1. Tsukimoto H. On an autopsied case of compression myelopathy with a callus formation in the cervical spinal canal. Nihon Geka Hokan. 1960;29:1003–7 (in Japanese).
2. Onji Y, Akiyama H, Shimomura Y, Ono K, Hukuda S, Mizuno S. Posterior paravertebral ossification causing cervical myelopathy. J Bone Jt Surg Am. 1967;49:1314–28.
3. Matsunaga S, Sakou T. OPLL: disease entity, incidence, literature search and prognosis. In: Yonenobu K, Nakamura K, Toyama Y, editors. Ossification of the posterior longitudinal ligament. 2nd ed. Tokyo: Springer; 2006. p. 11–7.
4. Inoue I. Genetic susceptibility to OPLL. In: Yonenobu K, Nakamura K, Toyama Y, editors. Ossification of the posterior longitudinal ligament. 2nd ed. Tokyo: Springer; 2006. p. 19–25.
5. Matsunaga S, Sakou T. Ossification of the posterior longitudinal ligament. In: Clark CR, editor. The cervical spine. 4th ed. Philadelphia: Lippincott Williams & Wilkins; 2005. p. 1091–8.
6. Tsuyama N. The investigation committee on OPLL of the Japanese Ministry of Public Health and Welfare. the ossification of the posterior longitudinal ligament of the spine (OPLL). J Jpn Orthop Assoc. 1981;55:425–40.
7. Sim J, Wright CC. The kappa statistic in reliability studies: use, interpretation, and sample size requirements. Phys Ther. 2005;85:257–68.
8. Karanicolas PJ, Bhandari M, Kreder H, Moroni A, Richardson M, Walter SD, Norman GR, Guyatt GH, Collaboration for outcome assessment in surgical trials (COAST) musculoskeletal group. Evaluating agreement: conducting a reliability study. J Bone Jt Surg Am. 2009;91(3 Suppl):99–106.
9. Kawaguchi Y, Nakano M, Yasuda T, Seki S, Hori T, Kimura T. Ossification of the posterior longitudinal ligament in not only cervical spine, but also other spinal regions: analysis using multidetector CT of the whole spine. Spine. 2013;38:E1477–82.
10. Fujimori T, Iwasaki M, Nagamoto Y, Kashii M, Ishii T, Sakaura H, Sugamoto K, Yoshikawa H. Three-dimensional measurement of intervertebral range of motion in ossification of the posterior longitudinal ligament: are there mobile segments in the continuous type? J Neurosurg Spine. 2012;17:74–81.
11. Matsunaga S, Kukita M, Hayashi K, Shinkura R, Koriyama C, Sakou T, Komiya S. Pathogenesis of myelopathy of patients with ossification of the posterior longitudinal ligament. J Neurosurg Spine. 2002;96(2 Suppl):168–72.
12. Matsunaga S, Nakamura K, Seichi A, Yokoyama T, Toh S, Ichimura S, Satomi K, Endo K, Yamamoto K, Kato Y, Ito T, Tokuhashi Y, Uchida K, Baba H, Kawahara N, Tomita K, Matsuyama Y, Ishiguro N, Iwasaki M, Yoshikawa H, Yonenobu K, Kawakami M, Yoshida M, Inoue S, Tani T, Kaneko K, Taguchi T, Imakiire T, Komiya S. Radiographic predictors for the development of myelopathy in patients with ossification of the posterior longitudinal ligament: a multicenter cohort study. Spine. 2008;33:2648–50.
13. Nagata K, Sato K. Diagnostic imaging of cervical ossification of the posterior longitudinal ligament. In: Yonenobu K, Nakamura K, Toyama Y, editors. Ossification of the posterior longitudinal ligament. 2nd ed. Tokyo: Springer; 2006. p. 127–43.

J Neurosurg Spine 21:417–424, 2014

In vivo 3D kinematic changes in the cervical spine after laminoplasty for cervical spondylotic myelopathy

Clinical article

Yukitaka Nagamoto, M.D., Ph.D.,[1] Motoki Iwasaki, M.D., Ph.D.,[1] Tsuyoshi Sugiura, M.D.,[1] Takahito Fujimori, M.D., Ph.D.,[1] Yohei Matsuo, M.D.,[1] Masafumi Kashii, M.D., Ph.D.,[1] Hironobu Sakaura, M.D., Ph.D.,[2] Takahiro Ishii, M.D., Ph.D.,[3] Tsuyoshi Murase, M.D., Ph.D.,[1] Hideki Yoshikawa, M.D., Ph.D.,[1] and Kazuomi Sugamoto, M.D., Ph.D.[1]

[1]Department of Orthopaedics, Osaka University Graduate School of Medicine, Suita, Osaka; [2]Department of Orthopaedic Surgery, Kansai Rosai Hospital, Amagasaki, Hyogo; and [3]Department of Orthopaedic Surgery, Kaizuka City Hospital, Kaizuka, Osaka, Japan

Object. Cervical laminoplasty is an effective procedure for decompressing the spinal cord at multiple levels, but restriction of neck motion is one of the well-known complications of the procedure. Although many authors have reported on cervical range of motion (ROM) after laminoplasty, they have focused mainly on 2D flexion and extension on lateral radiographs, not on 3D motion (including coupled motion) nor on precise intervertebral motion. The purpose of this study was to clarify the 3D kinematic changes in the cervical spine after laminoplasty performed to treat cervical spondylotic myelopathy.

Methods. Eleven consecutive patients (6 men and 5 women, mean age 68.1 years, age range 57–79 years) with cervical spondylotic myelopathy who had undergone laminoplasty were included in the study. All patients underwent 3D CT of the cervical spine in 5 positions (neutral, 45° head rotation left and right, maximum head flexion, and maximum head extension) using supporting devices. The scans were performed preoperatively and at 6 months after laminoplasty. Segmental ROM from Oc–C1 to C7–T1 was calculated both in flexion-extension and in rotation, using a voxel-based registration method.

Results. Mean C2–7 flexion-extension ROM, equivalent to cervical ROM in all previous studies, was 45.5° ± 7.1° preoperatively and 35.5° ± 8.2° postoperatively, which was a statistically significant 33% decrease. However, mean Oc–T1 flexion-extension ROM, which represented total cervical ROM, was 71.5° ± 8.3° preoperatively and 66.5° ± 8.3° postoperatively, an insignificant 7.0% decrease. In focusing on each motion segment, the authors observed a statistically significant 22.6% decrease in mean segmental ROM at the operated levels during flexion-extension and a statistically insignificant 10.2% decrease during rotation. The most significant decrease was observed at C2–3. Segmental ROM at C2–3 decreased 24.2% during flexion-extension and 21.8% during rotation. However, a statistically insignificant 37.2% increase was observed at the upper cervical spine (Oc–C2) during flexion-extension. The coupling pattern during rotation did not change significantly after laminoplasty.

Conclusions. In this first accurate documentation of 3D segmental kinematic changes after laminoplasty, Oc–T1 ROM, which represented total cervical ROM, did not change significantly during either flexion-extension or rotation by 6 months after laminoplasty despite a significant decrease in C2–7 flexion-extension ROM. This is thought to be partially because of a compensatory increase in segmental ROM at the upper cervical spine (Oc–C2).
(http://thejns.org/doi/abs/10.3171/2014.5.SPINE13702)

Key Words • **cervical laminoplasty** • **cervical spondylotic myelopathy** • **3D kinematics** • **volume registration** • **head rotation**

Cervical laminoplasty, a surgical alternative to laminectomy, is widely used to treat cervical spinal cord compression caused by cervical spondylosis or ossification of the posterior longitudinal ligament because it produces good long-term results.[12,22,28] Although laminoplasty has advantages such as a lower incidence of postoperative cervical kyphosis and preservation of range of motion (ROM), many authors have reported a significant decrease in cervical ROM after laminoplasty despite the good postoperative neurological improvements experienced by their patients.[1–6,11,12,15–18,20–22,25,26,28] However, they have investigated using only 2D flexion and extension on lateral radiographs. To our knowledge, there has been no report of 3D motion analysis about cervical laminoplasty, including coupled motion and precise intervertebral motion. Coupled motion is defined as combined motions that are mechanically forced to occur; it is difficult to measure it with conventional 2D methods.

For a better understanding of the precise pathophysiological change that occurs after laminoplasty, it is important to clarify the difference in precise kinematics before laminoplasty versus after it. We previously reported accurate in vivo 3D kinematics of the normal and degenerative

Abbreviations used in this paper: Oc = occiput; ROM = range of motion.

cervical spine using our own 3D motion-analysis method.[7–9,19] In the study we report here, we sought to accurately document 3D kinematic changes in the cervical spine after laminoplasty for cervical spondylotic myelopathy.

Methods

Our study included 11 consecutive patients (6 men and 5 women, mean age 68.1 years, age range 57–79 years) with cervical spondylotic myelopathy who had undergone open-door laminoplasty that used a modification of the Ito[10]-Tsuji[27] technique. In most patients, decompression extended from C-3 to C-6 or C-7. A full-thickness trough was drilled on one side of the lamina with a small bur and a high-speed drill. On the contralateral side, a partial-thickness trough was drilled. The lamina was then elevated toward the partial-thickness trough. The resected spinous process was placed into the space made after laminoplasty of C-4 and C-6 to keep the space open (Fig. 1). Of the 11 patients, 7 had disease that involved C3–6 and 4 had disease that involved C3–7. Patients with ossification of the posterior longitudinal ligament, diffuse idiopathic skeletal hyperostosis, rheumatoid arthritis, and trauma were excluded from the study. The duration of the period for which study participants wore a cervical collar after surgery ranged from 0 to 2 weeks. The average pre- and postoperative modified Japanese Orthopaedic Association scores were 10.7 ± 1.7 and 13.2 ± 1.6, respectively. The Hirabayashi recovery rate was 38.7% ± 20.3%.[3] All study protocols were approved by our institution's review board.

Acquisition of 3D CT Images

Computed tomography scans were obtained for 5 positions for each patient using a commercial CT system (LightSpeed VCT, GE Healthcare) with the following parameters: slice thickness 0.625 mm, pixel size 0.352 mm, tube rotation speed 0.5 seconds, beam collimation 40 mm, beam pitch 0.9, tube current 50 mA, and voltage 120 kV. Patients were placed in the supine position on the scanning table and in a neutral position, with their trunk at maximum flexion and extension and 45° axial rotation to the left and right achievable without pain or discomfort (Fig. 2). A supportive device was used to keep the head in flexion and rotation. When scanning patients with their trunk in extension, we took special care not to reproduce their neurological symptoms. The scans were performed before surgery and at 6 months after surgery. To reduce radiation exposure, scans done in positions other than neutral were performed with a lower tube current: 15 mA for rotation and extension and 30 mA only for flexion. Total exposure was 90 dose–length products, which is less than that specified for routine CT by our hospital, and CT data were transferred via a DICOM network into a computer workstation, where image processing was performed using Virtual Place software (M series, Medical Imaging Laboratory).

Motion Analysis

The method we used for motion analysis is fully described in our previous reports.[7–9,19] First, each vertebra was semi-automatically extracted using intensity threshold techniques. Second, the segmented images of the vertebrae in the neutral position were superimposed over images in other positions using voxel-based registration. As a result of this registration, the 3D migration of each vertebra was expressed by a matrix. Third, segmental motions from Oc–C1 to C7–T1 were calculated by converting the matrix obtained by the registration into a matrix representing relative motion with respect to the inferior adjacent vertebra both in flexion-extension and in rotation. Oc–T1 ROM (Oc motion relative to T-1, represented as total cervical ROM) and C2–7 ROM (C-2 motion relative to C-7, equivalent to a C2–7 angle measured on lateral radiographs) were also calculated. The results were expressed in 6 degrees of freedom by Euler angles, with the sequence of pitch (X), yaw (Y), and roll (Z), and in translations using a previously defined coordinate system[7–9,19] (Fig. 3). The ROM for flexion-extension was calculated as the sum of the flexion (+RX) and extension (–RX) angles, and the ROM for rotation was calculated as the sum of the right (–RY) and left (+RY) rotation angles. Coupled motion (lateral bending; ± RZ) during rotation was also

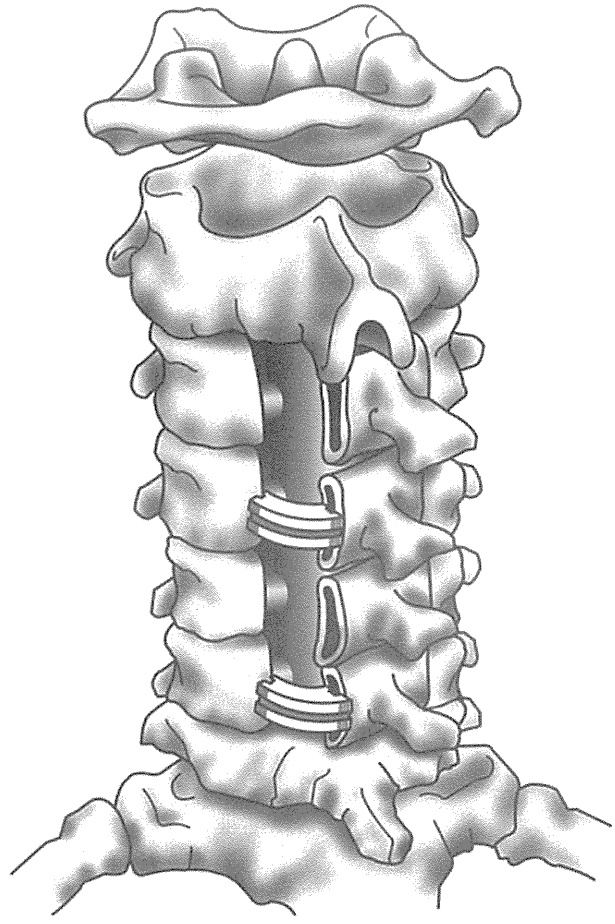

Fig. 1. Schematic illustration of the open-door laminoplasty technique that was used in this study, a modification of the Ito-Tsuji technique. Copyright Yukitaka Nagamoto. Published with permission.

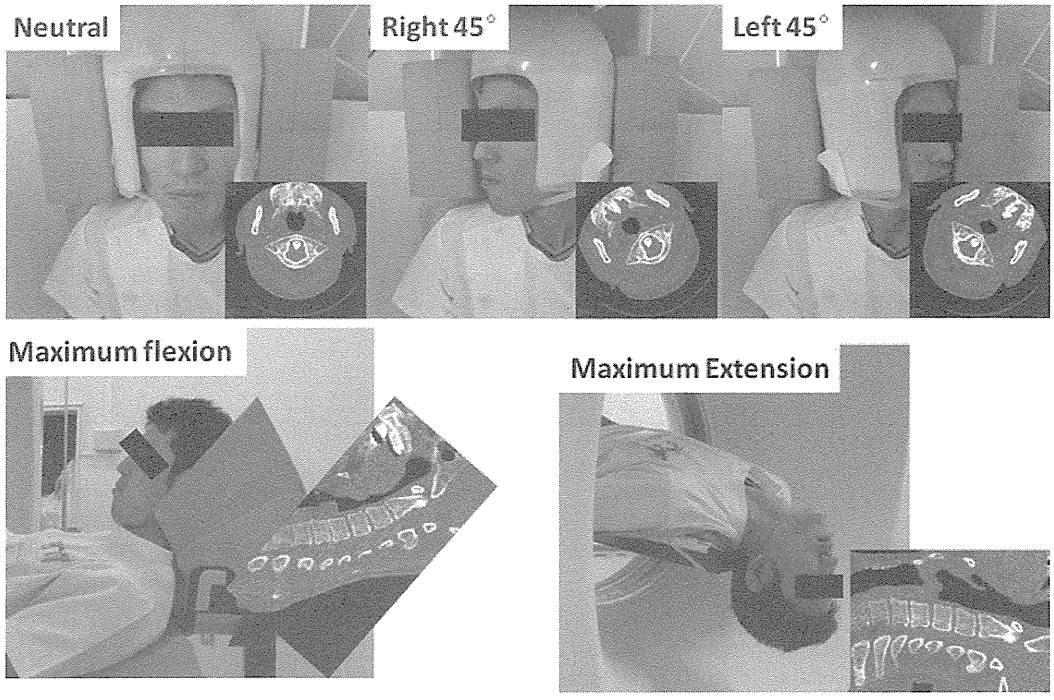

Fig. 2. Photographs and representative scans showing the 5 positions used for CT. Two types of supportive devices were used: one designed to facilitate production of the same 45° head rotation, and one to help maintain maximum flexion during scanning.

calculated as one-side motion. Vertebral slippage (± TZ) during flexion-extension was also measured from C2–3 to C7–T1. Vertebral slippage > 2.5 mm was defined as abnormal segmental motion.[1]

Accuracy Validation

We performed in vitro validation of the accuracy of our experimental CT method for the cervical spine using fresh-frozen vertebrae. More than 8 tantalum beads with a radius of 1.0 mm were implanted in the vertebrae. Subsequently, CT scans were performed 8 times in different positions with the same imaging parameters. Each vertebra was then superimposed by voxel-based registration. The true value of the migration was measured by marker-based registration, providing gold-standard data, and accuracy was defined as the closeness to the true value. The root mean square distance for migration was 0.19° in flexion-extension, 0.13° in axial rotation, 0.21° in lateral bending, 0.13 mm in lateral translation, 0.15 mm in superoinferior translation, and 0.31 mm in anteroposterior translation.

Statistical Analysis

All statistical analyses were performed with Excel 2007 for Windows XP (Microsoft) with the add-in software Statcel 2 (OMS Publishing Ltd.). The data were analyzed using the nonparametric Mann-Whitney U-test where indicated. A probability value of $p < 0.05$ was considered statistically significant.

Results

Oc–T1 and C2–7 Angle

Mean Oc–T1 flexion-extension ROM was 71.5° ± 8.3° preoperatively and 66.5° ± 8.3° postoperatively (Table 1; Fig. 4). Mean C2–7 flexion-extension ROM was 45.8° ± 8.3° preoperatively and 35.3° ± 8.2° postoperatively. Although C2–7 ROM decreased significantly ($p < 0.01$), total cervical ROM did not change significantly after laminoplasty during flexion-extension. Mean Oc–T1 rotation ROM was 83.7° ± 5.2° preoperatively and 79.8° ± 6.0° postoperatively. Mean C2–7 rotation ROM was 15.1° ± 4.4° preoperatively and 12.6° ± 3.1° postoperatively. Neither Oc–T1 nor C2–7 rotation ROM changed significantly after laminoplasty during rotation.

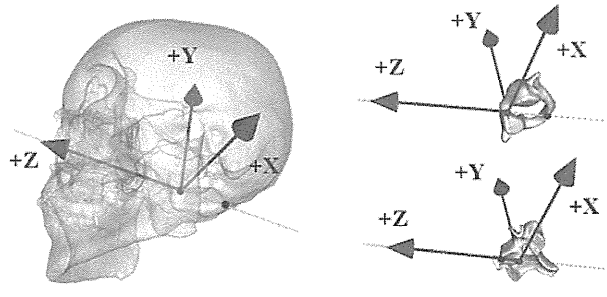

Fig. 3. Illustration of the anatomical orthogonal coordinate system as applied to the occiput (Oc), C-1, and subaxial vertebrae (C-5 shown).

TABLE 1: Segmental range of motion (°), means ± SD

Parameter	Oc–C1	C1–2	C2–3	C3–4	C4–5	C5–6	C6–7	C7–T1	Oc–T1	C2–7
flexion-extension										
preop	8.1 ± 8.9	8.1 ± 2.4	6.4 ± 2.5*	9.4 ± 5.1	11.7 ± 4.3	8.6 ± 3.8	9.8 ± 4.2	9.3 ± 2.7	71.5 ± 8.3	45.8 ± 7.1**
postop	12.5 ± 9.9	9.7 ± 3.9	3.9 ± 2.4*	6.9 ± 5.5	9.9 ± 4.4	5.9 ± 3.3	8.8 ± 4.5	8.6 ± 2.5	66.5 ± 8.3	35.3 ± 8.2**
rotation										
main motion										
preop	3.1 ± 2.0	54.4 ± 4.8	3.5 ± 1.5*	4.2 ± 2.1	4.8 ± 2.7	1.8 ± 1.5	1.1 ± 0.7	1.6 ± 0.9	83.7 ± 5.2	15.1 ± 4.4
postop	3.1 ± 1.4	52.8 ± 6.3	2.2 ± 1.2*	3.4 ± 2.1	4.4 ± 2.4	1.7 ± 1.7	1.2 ± 0.9	2.1 ± 0.9	79.8 ± 6.0	12.6 ± 3.1
coupled motion										
preop	−1.4 ± 0.8	−6.3 ± 2.4	3.6 ± 1.7	3.5 ± 1.9	3.0 ± 1.4	0.9 ± 0.7	0.7 ± 0.5	1.4 ± 0.9		
postop	−1.3 ± 0.9	−6.3 ± 2.5	2.3 ± 1.5	2.8 ± 2.0	2.8 ± 1.3	0.9 ± 0.6	0.8 ± 0.5	1.8 ± 1.1		

* $p < 0.05$.
** $p < 0.01$.

Segmental ROM During Flexion–Extension

Mean pre- and postoperative segmental ROM during flexion-extension were calculated (Table 1; Fig. 5). Segmental ROM decreased significantly at the proximal adjacent level (C2–3) and all operated levels (C3–6 laminoplasty, from C3–4 to C5–6; C3–7 laminoplasty, C3–4 to C6–7) ($p < 0.05$, Table 2). In compensation, segmental ROM tended to increase at the upper cervical levels (Oc–C1 and C1–2) during flexion-extension and at C7–T1 during rotation, but these increases were not statistically significant (Table 2). No new abnormal slippage occurred after laminoplasty. However, preoperative abnormal slippage, which was observed at only 1 segment, could not be decreased by laminoplasty (Fig. 6).

Segmental ROM During Rotation

Main Motion. The mean values for pre- and postoperative segmental ROM of main axial rotation during rotation were calculated (Table 1; Fig. 7). Segmental ROM decreased significantly at C2–3 and did not change significantly at the operated levels or the distal adjacent level (Table 2). No significant laterality of main motion was observed.

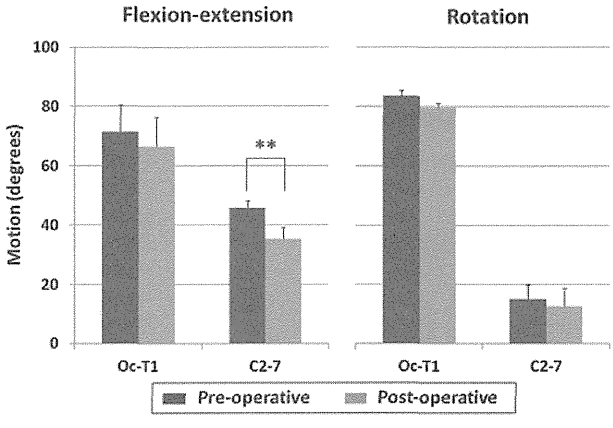

FIG. 4. Oc–T1 and C2–7 ROM before and after surgery, both in flexion-extension and in rotation. Oc–T1 ROM, represented as total cervical ROM, is the motion of the occiput relative to T-1. C2–7 ROM, equivalent to the C2–C7 angle measured on lateral radiographs, is the motion of C-2 relative to C-7. Data represent the mean ± SD. **$p < 0.01$.

Coupled Lateral Bending. The mean values for pre- and postoperative segmental ROM of coupled lateral bending during rotation were calculated (Table 1; Fig. 8). Coupled lateral bending during rotation was observed in the opposite direction at the upper cervical level and in the same direction at the subaxial spine, and this coupling pattern did not change after laminoplasty (Fig. 8). Although ROM showed no significant change after laminoplasty for any segment, only C2–3 segmental ROM had a strong tendency to decrease after laminoplasty (Table 2).

Discussion

Many researchers have reported that cervical ROM decreases significantly after laminoplasty.[1–6,11,13,15–18,20–22,25,26,28] According to a representative review by Ratliff and Cooper[20] of cervical laminoplasty, this decrease is an average of 50% (range 17%–80%). In one of the most recent reports, Hyun et al.[5] described a 20% decrease of ROM at 6 months after laminoplasty. However, almost all of these studies assessed neither total cervical ROM nor segmental ROM but only partial cervical flexion-extension ROM (C2–7 angle), using lateral radiographs.[1–6,11,13,15,16,18,21,22,26,28] That assessment method is useless when the C-7 vertebra is masked by shoulder girdle shadows. We obtained similar results in our study; we found that C2–7 ROM during flexion-extension decreased significantly by 23% after laminoplasty. Interestingly, however, we found little change in Oc–T1 ROM (total cervical ROM) because of a compensatory increase at the upper cervical spine (Oc–C2).

As for rotation ROM after laminoplasty, we found only 2 prior reports. Takeuchi et al.,[25] in evaluating cervical rotation using digital photographs, reported that rotational motion is significantly larger in laminoplasty that preserves the semispinalis cervicis inserted into C-2 than in conventional laminoplasty. Sugimoto et al.,[24] in evalu-

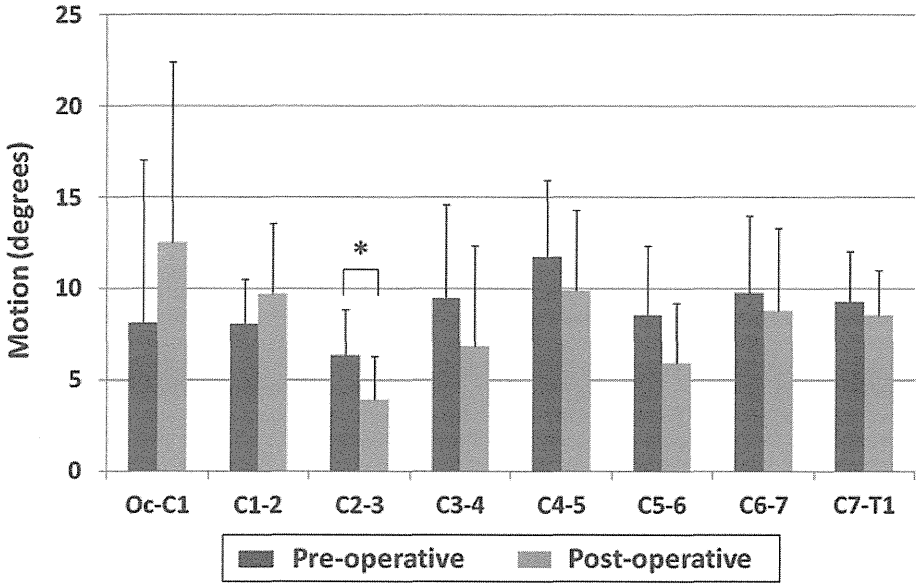

Fig. 5. Preoperative and postoperative segmental ROM in flexion-extension, Oc–C1 to C7–T1. *p < 0.05.

ating cervical rotation using 2D CT, reported that C1–T1 rotation ROM had not changed by 6 months after laminoplasty. Similarly, we found that neither Oc–T1 nor C2–7 rotation ROM changed significantly within the same head rotation angle. However, unlike previous studies, which investigated the change in total cervical ROM, our study mainly focused on the change in segmental kinematics, including coupled motion, within the same 45° head rotation angle after laminoplasty.

As for segmental ROM after laminoplasty, only Baba et al.[1] evaluated segmental ROM using flexion-extension lateral radiographs. They reported a significant decrease in ROM at all levels except C2–3 and C7–T1, based on values obtained at mean of 5.8 years after laminoplasty.[1] However, their data were unreliable because it is impossible to quantify small segmental ROM accurately on functional radiographs. No study has investigated segmental ROM during rotation after laminoplasty. Our precise measurements showed that segmental ROM at the operated levels was reduced significantly during flexion-extension and did not change significantly during rotation. Segmental ROM at C2–3, which is the proximal adjacent segment, showed the most significant decrease during both flexion-extension and rotation. At C2–3, as Iizuka et al.[6] suggested, the lifted C-3 lamina appeared to collide with the inferior edge of the C-2 lamina during both extension and rotation (see Videos 1 and 2, which demonstrate the reduction of ROM both in flexion-extension and in rotation by the collision of lifted laminae).

Video 1. Video clip showing a 3D animation of the C2–3 segment during flexion-extension. The left side of the video shows preoperative status; the right half shows postoperative status. Copyright Yukitaka Nagamoto. Published with permission. Click here to view with Media Player. Click here to view with Quicktime.

Video 2. Video clip showing a 3D animation of the C2–C3 segment during rotation. The left side of the video shows preoperative status; the right half shows postoperative status. Copyright Yukitaka Nagamoto. Published with permission. Click here to view with Media Player. Click here to view with Quicktime.

We think that this is the mechanism by which the segmental ROM at C2–3 decreased omnidirectionally and that this is one of reasons C2–3 is the level most frequently involved in laminar fusion.[6,22,28]

No study has investigated coupled motion in the cervical spine after laminoplasty. Normal coupled lateral bending during rotation occurs in the opposite direction at the upper cervical level and in the same direction at the subaxial spine, and coupled motion is thought to be driven by the oblique orientation of the apophyseal joint.[8,9] In our

TABLE 2: Summary of segmental range of motion change after laminoplasty†

Level	Cervical Level	Flexion-Extension	Rotation: MM	Rotation: CM
upper	Oc–C2	37.2% (p = 0.146)	−13.0% (p = 0.370)	−1.4% (p = 0.999)
PA	C2–3	−24.2%* (p = 0.039)	−21.8%* (p = 0.028)	−16.2% (p = 0.082)
operated	C3–6 or C3–7	−22.6%* (p = 0.023)	−10.2% (p = 0.600)	−16.8% (p = 0.262)
DA	C6–7 or C7–T1	−8.4% (p = 0.674)	7.1% (p = 0.870)	−5.1% (p = 0.597)

* p < 0.05.

† CM = coupled motion; DA = distal adjacent level; MM = main motion; PA = proximal adjacent level; upper = upper cervical level.

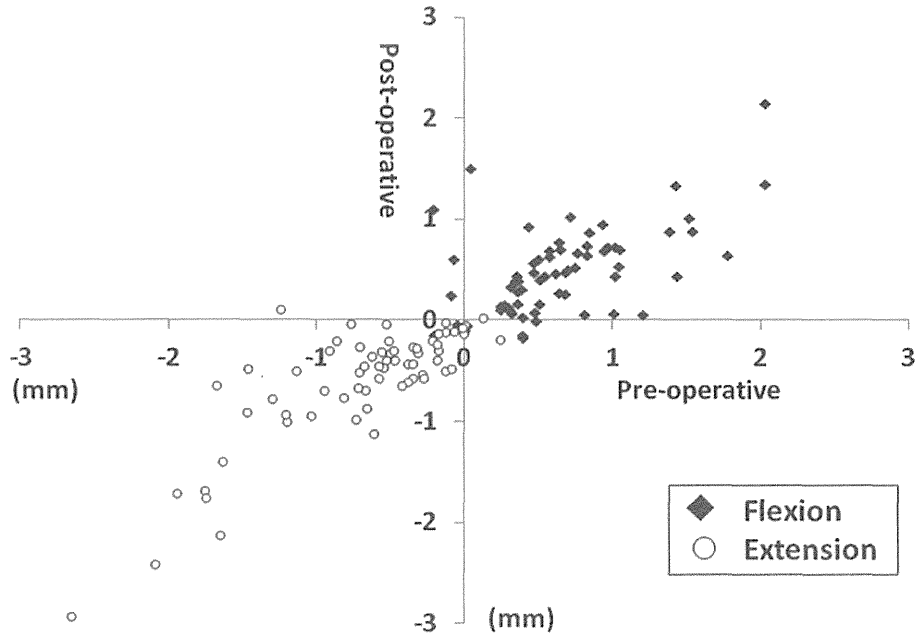

Fig. 6. Vertebral slippage during flexion-extension (horizontal axis, preoperative; vertical axis, postoperative). A positive value indicates anterior slippage, and a negative value indicates posterior slippage.

study, we observed a normal coupled pattern both before and after surgery. This is because cervical laminoplasty can preserve the apophyseal joint, which drives coupled motion.

None of our study participants had abnormal slippage after surgery or deterioration of a preexisting slip as early as 6 months after laminoplasty despite early postoperative removal of cervical collars. Postoperative segmental ROM tended to be reduced more severely at the middle cervical levels (from C2–3 to C4–5) than at the lower cervical levels (from C5–6 to C7–T1) (Figs. 5, 7, and 8). Shigematsu et al.[23] reported that 87% of cervical degenerative spondylolisthesis had stabilized after laminoplasty, and Kawasaki et al.[14] reported that in 93% of cases, degenerative spondylolisthesis occurred at C3–4 or C4–5. Given our results, we believe that cervical laminoplasty preserves cervical ROM without harmful intervertebral instability and is a reasonable and beneficial procedure for the treatment of elderly patients with myelopathy who have degenerative spondylolisthesis of the middle cervical spine.

In our study, total cervical kinematics had not changed significantly during either flexion-extension or rotation by

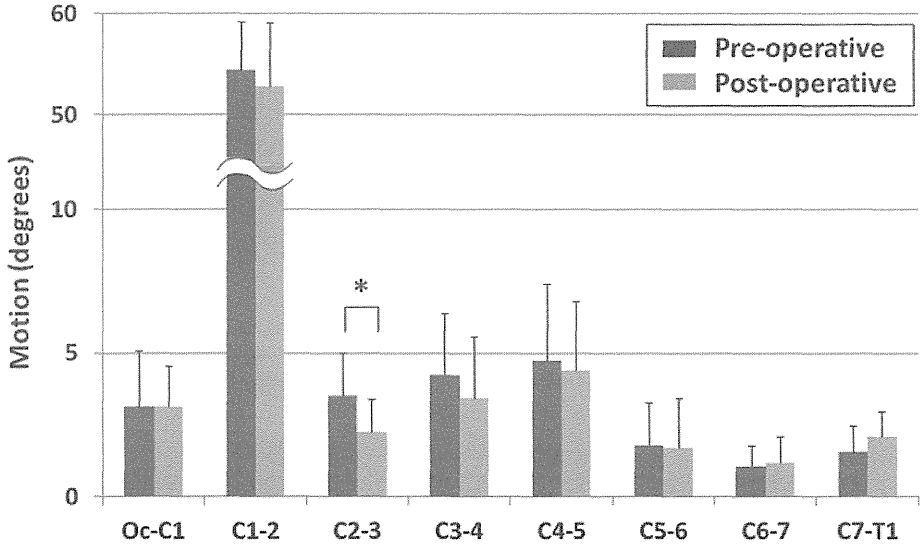

Fig. 7. Preoperative and postoperative segmental range of motion for main axial rotation during rotation, Oc–C1 to C7–T1. *$p < 0.05$.

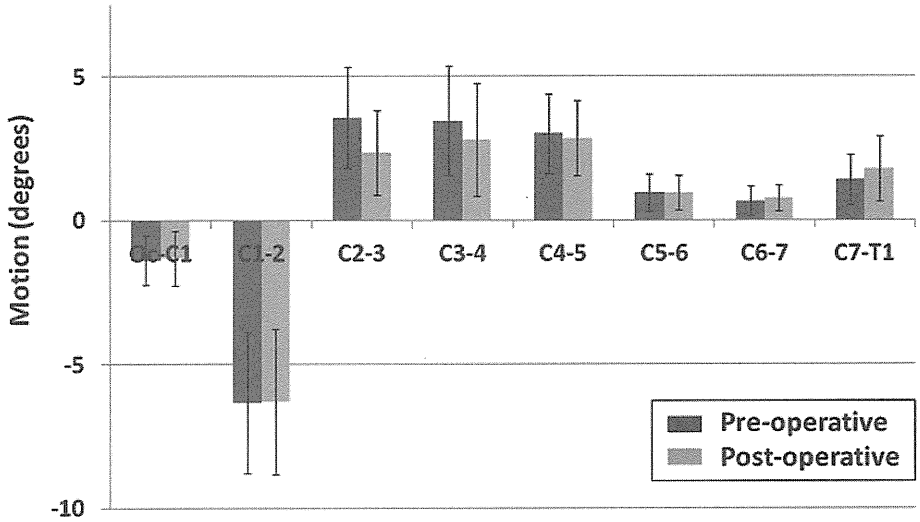

FIG. 8. Preoperative and postoperative segmental range of motion for coupled lateral bending during rotation, Oc–C1 to C7–T1. The negative values represent contralateral bending. For example: During right head rotation, ipsilateral bending (right side bending) occurs at C2–3, C3–4, C4–5, C5–6, C6–7, and C7–T1 and contralateral bending (left side bending) occurs at Oc–C1 and C1–2.

6 months after laminoplasty. Actually, no patient in our study reported loss of neck motion. In addition, we have never encountered any patients reporting disabling loss of neck motion after laminoplasty. This may be explained by early removal of cervical collars, postoperative neck exercises, and some surgical modifications in comparison with procedures performed from the late 1990s to the early years of the 21st century.[1,3,13,16,22,28] Meanwhile, Hyun et al.[5] reported that post-laminoplasty cervical ROM continues to decrease for up to 18 months after surgery. Therefore, a follow-up kinematic study of cervical laminoplasty over the long term will provide more conclusive results.

Conclusions

We produced the first accurate documentation of 3D segmental kinematic changes after laminoplasty. At 6 months after laminoplasty, C2–7 flexion-extension ROM, equivalent to cervical ROM in all previous studies, showed a statistically significant 33% decrease, a result similar to that of previous studies. In focusing on each motion segment, we found that the most significant decrease occurred at C2–3, both during flexion-extension and rotation. However, we observed a statistically insignificant 37.2% increase at the upper cervical spine (Oc–C2) during flexion-extension. Oc–T1 ROM, which represented total cervical ROM, showed an insignificant 7% decrease in flexion-extension and an insignificant 4% decrease in rotation despite the significant decrease in C2–7 flexion-extension ROM. This is thought to be partly because of a compensatory increase in segmental ROM at the upper cervical spine.

Acknowledgments

We thank Ryoji Nakao for assisting with software programming and Shinichiro Hirose for help with CT imaging. We also acknowledge the contribution of medical editor Katharine O'Moore-Klopf, ELS (East Setauket, New York), who provided professional English-language editing of this article.

Disclosure

This work was supported by a grant-in-aid for Scientific Research C (KAKENHI:22591632) from the Ministry of Education, Culture, Sports and Technology, Japan. The authors report that no benefits in any form have been or will be received from any commercial party related directly or indirectly to the subject of this study.

Author contributions to the study and manuscript preparation include the following. Conception and design: Nagamoto, Iwasaki. Acquisition of data: Nagamoto, Sugiura, Matsuo. Analysis and interpretation of data: Nagamoto, Fujimori. Drafting the article: Nagamoto. Critically revising the article: all authors. Reviewed submitted version of manuscript: all authors. Approved the final version of the manuscript on behalf of all authors: Nagamoto. Statistical analysis: Nagamoto. Administrative/technical/material support: Iwasaki, Kashii, Murase, Yoshikawa, Sugamoto. Study supervision: Iwasaki, Yoshikawa, Sugamoto.

References

1. Baba H, Maezawa Y, Furusawa N, Imura S, Tomita K: Flexibility and alignment of the cervical spine after laminoplasty for spondylotic myelopathy. A radiographic study. **Int Orthop 19:**116–121, 1995
2. Fujimori T, Le H, Ziewacz JE, Chou D, Mummaneni PV: Is there a difference in range of motion, neck pain, and outcomes in patients with ossification of posterior longitudinal ligament versus those with cervical spondylosis, treated with plated laminoplasty? **Neurosurg Focus 35(1):**E9, 2013
3. Heller JG, Edwards CC II, Murakami H, Rodts GE: Laminoplasty versus laminectomy and fusion for multilevel cervical myelopathy: an independent matched cohort analysis. **Spine (Phila Pa 1976) 26:**1330–1336, 2001
4. Highsmith JM, Dhall SS, Haid RW Jr, Rodts GE Jr, Mummaneni PV: Treatment of cervical stenotic myelopathy: a cost and outcome comparison of laminoplasty versus laminectomy and lateral mass fusion. Clinical article. **J Neurosurg Spine 14:**619–625, 2011

5. Hyun SJ, Rhim SC, Roh SW, Kang SH, Riew KD: The time course of range of motion loss after cervical laminoplasty: a prospective study with minimum two-year follow-up. **Spine (Phila Pa 1976) 34:**1134–1139, 2009
6. Iizuka H, Iizuka Y, Nakagawa Y, Nakajima T, Toda N, Shimegi A, et al: Interlaminar bony fusion after cervical laminoplasty: its characteristics and relationship with clinical results. **Spine (Phila Pa 1976) 31:**644–647, 2006
7. Ishii T, Mukai Y, Hosono N, Sakaura H, Fujii R, Nakajima Y, et al: Kinematics of the cervical spine in lateral bending: in vivo three-dimensional analysis. **Spine (Phila Pa 1976) 31:** 155–160, 2006
8. Ishii T, Mukai Y, Hosono N, Sakaura H, Fujii R, Nakajima Y, et al: Kinematics of the subaxial cervical spine in rotation in vivo three-dimensional analysis. **Spine (Phila Pa 1976) 29:**2826–2831, 2004
9. Ishii T, Mukai Y, Hosono N, Sakaura H, Nakajima Y, Sato Y, et al: Kinematics of the upper cervical spine in rotation: in vivo three-dimensional analysis. **Spine (Phila Pa 1976) 29:**E139–E144, 2004
10. Itoh T, Tsuji H: Technical improvements and results of laminoplasty for compressive myelopathy in the cervical spine. **Spine (Phila Pa 1976) 10:**729–736, 1985
11. Kang SH, Rhim SC, Roh SW, Jeon SR, Baek HC: Postlaminoplasty cervical range of motion: early results. **J Neurosurg Spine 6:**386–390, 2007
12. Kawaguchi Y, Kanamori M, Ishihara H, Ohmori K, Nakamura H, Kimura T: Minimum 10-year followup after en bloc cervical laminoplasty. **Clin Orthop Relat Res (411):**129–139, 2003
13. Kawaguchi Y, Matsui H, Ishihara H, Gejo R, Yasuda T: Surgical outcome of cervical expansive laminoplasty in patients with diabetes mellitus. **Spine (Phila Pa 1976) 25:**551–555, 2000
14. Kawasaki M, Tani T, Ushida T, Ishida K: Anterolisthesis and retrolisthesis of the cervical spine in cervical spondylotic myelopathy in the elderly. **J Orthop Sci 12:**207–213, 2007
15. Kimura I, Shingu H, Nasu Y: Long-term follow-up of cervical spondylotic myelopathy treated by canal-expansive laminoplasty. **J Bone Joint Surg Br 77:**956–961, 1995
16. Maeda T, Arizono T, Saito T, Iwamoto Y: Cervical alignment, range of motion, and instability after cervical laminoplasty. **Clin Orthop Relat Res (401):**132–138, 2002
17. Matz PG, Anderson PA, Groff MW, Heary RF, Holly LT, Kaiser MG, et al: Cervical laminoplasty for the treatment of cervical degenerative myelopathy. **J Neurosurg Spine 11:**157–169, 2009
18. Meyer SA, Wu JC, Mummaneni PV: Laminoplasty outcomes: is there a difference between patients with degenerative stenosis and those with ossification of the posterior longitudinal ligament? **Neurosurg Focus 30(3):**E9, 2011
19. Nagamoto Y, Ishii T, Sakaura H, Iwasaki M, Moritomo H, Kashii M, et al: In vivo three-dimensional kinematics of the cervical spine during head rotation in patients with cervical spondylosis. **Spine (Phila Pa 1976) 36:**778–783, 2011
20. Ratliff JK, Cooper PR: Cervical laminoplasty: a critical review. **J Neurosurg 98 (3 Suppl):**230–238, 2003
21. Satomi K, Nishu Y, Kohno T, Hirabayashi K: Long-term follow-up studies of open-door expansive laminoplasty for cervical stenotic myelopathy. **Spine (Phila Pa 1976) 19:**507–510, 1994
22. Seichi A, Takeshita K, Ohishi I, Kawaguchi H, Akune T, Anamizu Y, et al: Long-term results of double-door laminoplasty for cervical stenotic myelopathy. **Spine (Phila Pa 1976) 26:**479–487, 2001
23. Shigematsu H, Ueda Y, Takeshima T, Koizumi M, Satoh N, Matsumori H, et al: Degenerative spondylolisthesis does not influence surgical results of laminoplasty in elderly cervical spondylotic myelopathy patients. **Eur Spine J 19:**720–725, 2010 (Erratum in **Eur Spine J 19:**1393, 2010)
24. Sugimoto Y, Tanaka M, Nakanishi K, Misawa H, Takigawa T, Ikuma H, et al: Assessing range of cervical rotation after laminoplasty using axial CT. **J Spinal Disord Tech 20:**187–189, 2007
25. Takeuchi K, Yokoyama T, Ono A, Numasawa T, Wada K, Kumagai G, et al: Cervical range of motion and alignment after laminoplasty preserving or reattaching the semispinalis cervicis inserted into axis. **J Spinal Disord Tech 20:**571–576, 2007
26. Tomita K, Kawahara N, Toribatake Y, Heller JG: Expansive midline T-saw laminoplasty (modified spinous process-splitting) for the management of cervical myelopathy. **Spine (Phila Pa 1976) 23:**32–37, 1998
27. Tsuji H: Laminoplasty for patients with compressive myelopathy due to so-called spinal canal stenosis in cervical and thoracic regions. **Spine (Phila Pa 1976) 7:**28–34, 1982
28. Wada E, Suzuki S, Kanazawa A, Matsuoka T, Miyamoto S, Yonenobu K: Subtotal corpectomy versus laminoplasty for multilevel cervical spondylotic myelopathy: a long-term follow-up study over 10 years. **Spine (Phila Pa 1976) 26:**1443–1448, 2001

Manuscript submitted July 29, 2013.
Accepted May 6, 2014.
Portions of this study were presented in the podium session at the 39th Annual Meeting of the Cervical Spine Research Society, Scottsdale, Arizona, December 8–10, 2011.
Please include this information when citing this paper: published online June 13, 2014; DOI: 10.3171/2014.5.SPINE13702.

Supplemental online information:

Video 1: http://mfile.akamai.com/21490/wmv/digitalwbc.download.akamai.com/21492/wm.digitalsource-na-regional/spine13-702_video_1.asx (Media Player).
http://mfile.akamai.com/21488/mov/digitalwbc.download.akamai.com/21492/qt.digitalsource-global/spine13-702_video_1.mov (Quicktime).
Video 2: http://mfile.akamai.com/21490/wmv/digitalwbc.download.akamai.com/21492/wm.digitalsource-na-regional/spine13-702_video_2.asx (Media Player).
http://mfile.akamai.com/21488/mov/digitalwbc.download.akamai.com/21492/qt.digitalsource-global/spine13-702_video_2.mov (Quicktime).

Address correspondence to: Yukitaka Nagamoto, M.D., Ph.D., Department of Orthopaedic Surgery, Osaka National Hospital, 2-1-14 Hoenzaka, Osaka 540-0006, Japan. email: 7gam0to@gmail.com.

Chapter 3
Autophagy in Spinal Cord Injury: Pathogenic Roles and Therapeutic Implications

Autophagy in Spinal Cord Injury

Haruo Kanno and Hiroshi Ozawa

Abstract Autophagy is degradation of intracellular proteins and organelles to maintain cytoplasmic homeostasis, and it is also involved in various pathophysiological processes in many diseases. We previously investigated alternation of autophagic activity in damaged neural tissue after SCI. It was also examined whether administration of rapamycin to promote autophagy can induce neuroprotective effect in SCI. Our results of these studies demonstrated that molecular markers of autophagy such as Beclin 1 and LC3 were significantly upregulated in the injured spinal cord. The increased activity of autophagy was observed in neurons, astrocytes, and oligodendrocytes at the lesion site. Electron microscopy showed an increased formation of autophagic vacuoles in the damaged neural cells. In addition, the rapamycin administration in acute phase of SCI promoted autophagy in the injured spinal cord and reduced neural tissue damage and locomotor impairment. These findings indicated that autophagic activity is increased in damaged neural tissue after SCI. Furthermore the promotion of autophagy by rapamycin treatment can provide neuroprotective effect to improve locomotor function following SCI. Here, we summarize our previous studies and review the evidence in related articles regarding the role of autophagy in SCI.

Keywords Autophagy • Beclin 1 • LC3 • Rapamycin • Spinal cord injury

H. Kanno (✉) • H. Ozawa
Department of Orthopaedic Surgery, Tohoku University School of Medicine,
1-1 Seiryo-machi, Aoba-ku, Sendai 980-8574, Japan
e-mail: kanno-h@isis.ocn.ne.jp

K. Uchida et al. (eds.), *Neuroprotection and Regeneration of the Spinal Cord*,
DOI 10.1007/978-4-431-54502-6_3, © Springer Japan 2014

3.1 Introduction

Autophagy is degradation of intracellular proteins and organelles to maintain cytoplasmic homeostasis, and it is also involved in various pathophysiological processes in many diseases [1–4]. Autophagy works for the elimination and recycling of long-lived proteins and unwanted organelles in a cell during development and under stress conditions [1, 5, 6] (Fig. 3.1). Amino acid starvation is a well-known trigger for autophagy, which degrades proteins to free amino acids that help cell survival [2].

Previous studies suggested that autophagy has a cytoprotective function against cell death [7, 8]. Autophagy contributed to cytoprotection in neurodegenerative disease and traumatic brain injury [9–13]. On the contrary, previous studies suggested that autophagy also contributes to the induction of cell death [8, 14, 15]. Autophagy can lead to nonapoptotic programmed cell death, which is called autophagic cell death [3, 16]. Activation of autophagy can induce cell death in a myocardial ischemia and reperfusion model [17]. In addition, autophagy can lead to autophagic cell death in cerebral ischemia and in a renal ischemia and reperfusion injury [18, 19].

Beclin 1, a Bcl-2-interacting protein, is a mammalian ortholog of yeast Atg6/Vps30 and it is known to be a promoter of autophagy [20]. Beclin 1 is a component of the class III phosphatidylinositol-3-kinase (PI3K) complex that works for the formation of autophagosomes [21]. The Atg8 protein, known as microtubule-associated protein 1 light chain 3 (LC3), is essential for autophagy [22]. LC3 is bound to autophagosomal membrane and thus is considered a specific marker protein to monitor autophagy [23] (Fig. 3.1). Autophagy may be dysregulated in several disorders, including metabolic diseases, neurodegenerative disorders, infectious diseases, and cancer. Pharmacological approaches to upregulate or inhibit this pathway are currently receiving considerable attention [24]. The mammalian target of rapamycin (mTOR) signaling pathway is known as a main molecular mechanism to

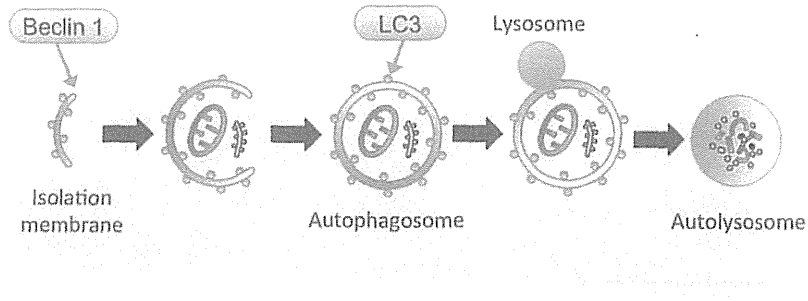

Fig. 3.1 Process of autophagy. A small volume of cytoplasm is enclosed by the isolation membrane, which results in the formation of an autophagosome. The autophagosome fuses with the lysosome where the cytoplasm is degraded. LC3 is bound to the autophagosomal membrane

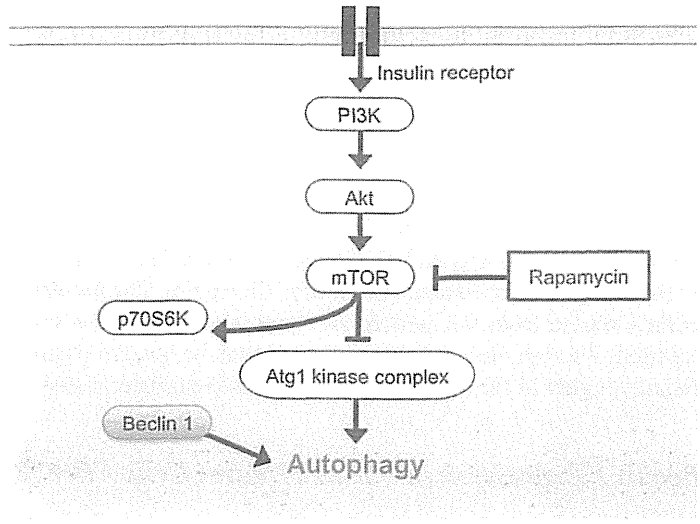

Fig. 3.2 Signaling pathway of autophagy regulation. mTOR pathway negatively regulates autophagy. Rapamycin, a specific inhibitor of mTOR, prevents phosphorylation of p70S6K and promotes autophagy. Beclin 1 protein promotes autophagy

regulate autophagic activity (Fig. 3.2). Recent studies revealed modulation of autophagy via mTOR signaling can be a therapeutic target for various diseases [24].

We previously reported that autophagic activity was upregulated in damaged neural tissue after SCI [25–27]. Furthermore our study demonstrated that pharmacological enhancement of autophagy provided neuroprotective effect following SCI [28, 29]. Here, we summarize our previous studies and review the evidence in related articles regarding the role of autophagy in SCI.

3.2 Upregulation of Beclin 1 Expression After Spinal Cord Injury

3.2.1 Summary

Beclin 1, a Bcl-2-interacting protein, is known to be a promoter of autophagy. We previously investigated the alterations in the Beclin 1 protein expression and the involvement of autophagy after SCI using a spinal cord hemisection model in mice [25]. In our results of immunohistochemistry and Western blot analysis, the Beclin 1 expression significantly increased at the lesion site after hemisection. The Beclin 1 expression was observed in neurons, astrocytes, and oligodendrocytes. These results suggested that autophagy can be activated in the injured spinal cord.

3.2.2 *Increased Expression of Beclin 1 After SCI*

To investigate an alteration of the Beclin 1 expression in the spinal cord, immunohistochemical staining of Beclin 1 was performed at 4 and 24 h and 3, 7, and 21 days after hemisection. The cells expressing Beclin 1 were increased in the injured side after hemisection (Fig. 3.3a). The cells expressing Beclin 1 were observed in both the gray matter and white matter of the injured side. In counting Beclin 1-positive cells, the number of Beclin 1-positive cells on the injured side was significantly higher than those on the contralateral side at each time point. The increased expression of Beclin 1 started from 4 h, peaked at 3 days, and lasted for at least 21 days after hemisection. Western blot analysis confirmed that the level of Beclin 1 protein was significantly higher in the injured side than in the contralateral side.

3.2.3 *Beclin 1 Expression in Various Neural Cells After SCI*

To investigate the Beclin 1 expression in a specific type of cells including neurons, astrocytes, and oligodendrocytes, the spinal cord sections at 3 days after hemisection were double stained for Beclin 1 and various cell type markers: NeuN for neurons, GFAP for astrocytes, and Olig2 for oligodendrocytes. In the double staining, the expression of Beclin 1 was observed in NeuN-, GFAP-, and Olig2-labeled cells. These results demonstrated the Beclin 1 expression to be observed in neurons, astrocytes, and oligodendrocytes.

3.2.4 *Expression of Beclin 1 in Dying Cells*

To detect Beclin 1 expression in dying cells, we performed double staining of Beclin 1 and TUNEL in the sections at 3 days after hemisection. The TUNEL-positive cells occasionally showed as Beclin 1 positive. Under higher magnification, most of the nuclei of the TUNEL-positive cells that did not show Beclin 1 positive were shrunken or fragmented, as is typical of apoptotic nuclei. On the other hand, most of the nuclei of the TUNEL-positive cells that were found to be Beclin 1 positive were round, as in autophagic cell death, and they had neither shrunken nor were fragmented.

3.3 Confirmation of Autophagy Induction After Spinal Cord Injury

3.3.1 *Summary*

To confirm induction of autophagy after SCI, we previously investigated expression of LC3, a characteristic marker of autophagy, in immunohistochemistry and Western blot using an SCI model in mice [26]. Electron microscopic analysis was

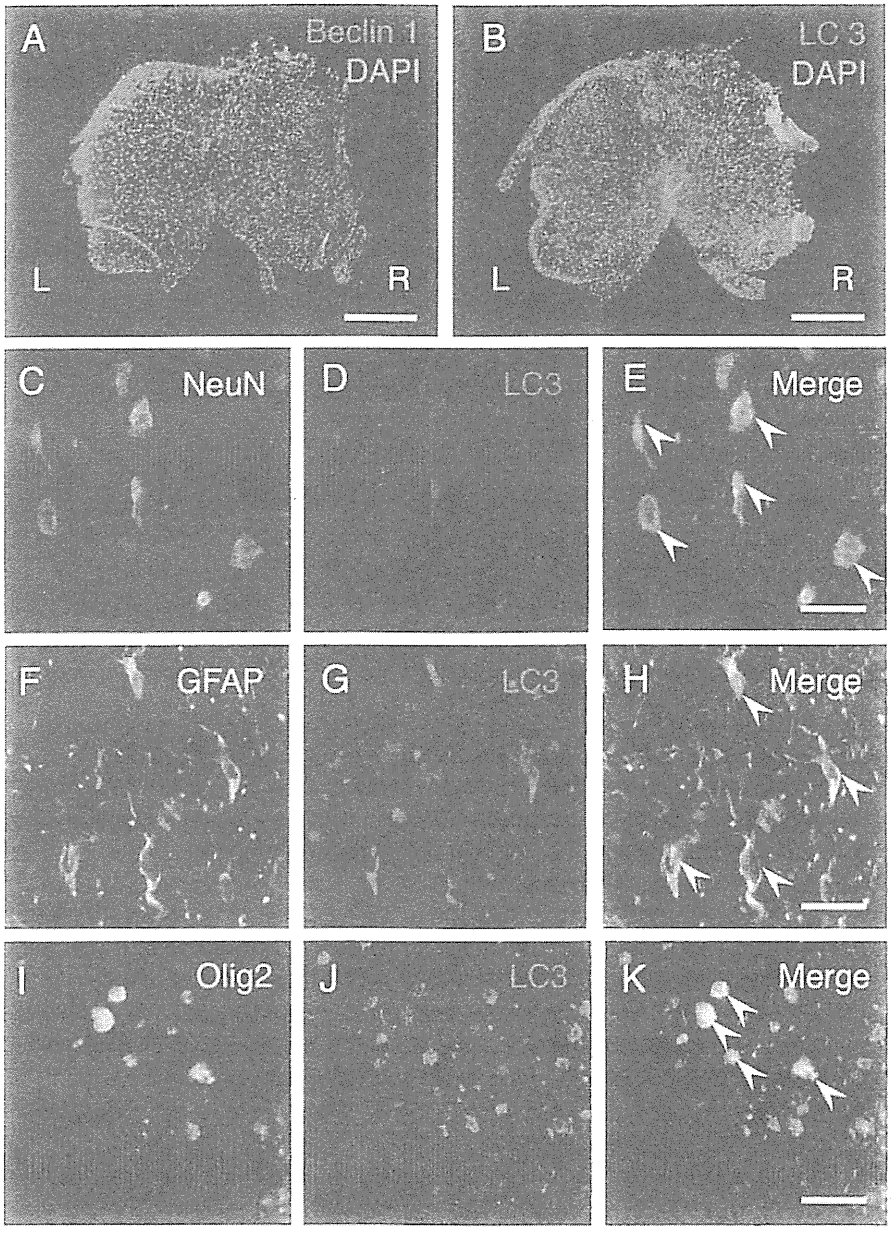

Fig. 3.3 Immunohistochemical staining of Beclin1 and LC3 in transverse sections at 3 days after hemisection. (**a**), (**b**) The cells expressing Beclin1 and LC3 were increased on the injured side (R) in comparison to the contralateral side (L). Scale bars = 500 μm. (**c**)–(**k**) In double staining of LC3 and cell type makers (*green*) on the injured side in transverse section at 3 days after hemisection, the LC3-positive cells were observed in the NeuN-, GFAP-, and Olig2-labeled cells (*arrowheads* in (**e**), (**h**), (**k**)). Scale bars = 50 μm

also performed to examine the formation of autophagy in the injured spinal cord. Immunohistochemistry showed that the number of the LC3-positive cells significantly increased at the lesion site after hemisection. The LC3-positive cells were observed in neurons, astrocytes, and oligodendrocytes. Western blot analysis demonstrated that the level of LC3-II protein expression significantly increased in the injured spinal cord. Electron microscopy showed an increased formation of autophagic vacuoles in the damaged neural cells. This study confirmed both biochemically and anatomically that autophagy was clearly activated in the damaged neural tissue after SCI.

3.3.2 *Upregulation of Autophagy Marker, LC3 in Injured Spinal Cord*

Immunohistochemical analysis showed that cells expressing LC3 were increased on the injured side in comparison to the contralateral side after hemisection. The cells expressing LC3 were observed in both the gray matter and the white matter of the injured side (Fig. 3.3b). In higher magnification on the injured side, the cells expressing LC3 displayed bright, punctate LC3 dots in the cytoplasm, indicating formation of autophagic vacuoles. The number of LC3-positive cells on the injured side was significantly higher than those on the contralateral side at 3 days. The increase of the LC3-positive cells commenced at 4 h and lasted for at least 21 days. The maximum number of LC3-positive cells on the injured side was observed at 3 days, and it thereafter decreased at 7 days after hemisection. Western blot analysis confirmed the level of LC3-II protein was significantly higher in the injured side than in uninjured spinal cord.

3.3.3 *LC3 Expression in Various Neural Cells*

Double staining of LC3 and various cell type markers revealed that the LC3-positive cells were observed in NeuN-, GFAP-, and Olig2-labeled cells on the injured side after hemisection (Fig. 3.3c–k).

3.3.4 *Electron Microscopic Analysis for Autophagy Formation*

Electron microscopic analysis after the hemisection demonstrated that the formations of numerous autophagic vacuoles including autophagosome with double-membrane structures (Fig. 3.1) were observed in the damaged cells on the injured side. A higher magnification showed that the autophagosomes were containing membranous structures and parts of the cytoplasm.

3.3.5 Expression of LC3 in Dying Cells

To confirm autophagy induction in dying cells, we performed double staining of LC3 and TUNEL using the spinal cord section at 3 days after hemisection. The double staining showed that the TUNEL-positive cells were occasionally LC3 positive. Higher magnification revealed that the nuclei of the TUNEL-positive cells that were not LC3 positive were shrunken or fragmented, typical of apoptotic nuclei. On the contrary, the nuclei of the TUNEL-positive cells that were found to be LC3 positive were round, as in autophagic cell death.

3.4 Autophagy Modulation as a Potential Therapeutic Target for Spinal Cord Injury

3.4.1 Summary

The mTOR is a serine/threonine kinase that negatively regulates autophagy (Fig. 3.2). Rapamycin, an inhibitor of mTOR signaling, can promote autophagy and exert neuroprotective effects in several diseases of the central nervous system. We previously investigated whether administration of rapamycin promotes autophagy and reduces neural tissue damage and locomotor impairment after spinal cord contusion injury in mice [28]. Our results demonstrated that the administration of rapamycin at 4 h after injury significantly promoted autophagic activity in the injured spinal cord. In addition, the rapamycin treatment significantly reduced neural tissue damage and locomotor impairment after SCI. These results indicate that rapamycin promoted autophagy by inhibiting the mTOR signaling pathway and induced neuroprotective effect after SCI (Fig. 3.4).

3.4.2 Inhibition of mTOR Promotes Autophagy After Spinal Cord Injury

To examine the effectiveness of the rapamycin treatment on the mTOR signaling pathway, the phosphorylation of p70S6K was evaluated by Western blot analysis. In our results, the phosphorylated p70S6K protein was significantly decreased after administration of rapamycin, indicating rapamycin actually inhibited mTOR after SCI (Fig. 3.4). We also investigated the activation of autophagy after rapamycin treatment, immunohistochemical staining, and Western blot analysis of LC3 were performed. Immunostaining of LC3 showed the number of LC3-positive cells was significantly increased in the rapamycin-treated mice compared with the vehicle-treated mice. In the Western blot analysis, the expression of LC3-II protein was significantly increased in the rapamycin-treated mice compared with the vehicle-treated mice.

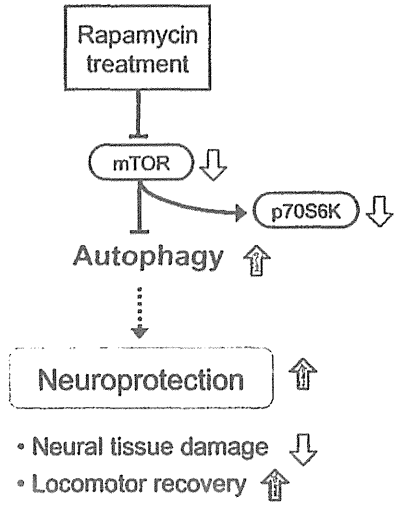

Fig. 3.4 Neuroprotective mechanism of rapamycin treatment in acute SCI. Rapamycin suppresses mTOR signaling pathway and promotes autophagy after SCI. The increased autophagic activity can produce neuroprotective effect and reduce neural tissue damage and locomotor impairment following SCI

3.4.3 Inhibition of mTOR Produces Neuroprotective Effect in Injured Spinal Cord

To investigate neural cell loss after injury, the number of NeuN-positive cells was compared between the vehicle and the rapamycin-treated mice by immunohistochemical staining. In our results, the number of NeuN-positive cells in the rapamycin-treated mice was significantly higher than those in the vehicle-treated mice at 42 days. Additionally, to investigate the effect of rapamycin on cell death after SCI, we performed TUNEL staining and compared the number of TUNEL-positive cells between the vehicle- and the rapamycin-treated mice at 3 days after injury. The number of TUNEL-positive cells was significantly lower in the rapamycin-treated mice compared to the vehicle-treated mice. These results indicated that rapamycin treatment can produce neuroprotective effect to reduce neuronal loss and cell death following SCI.

3.4.4 Inhibition of mTOR Improves Locomotor Recovery After Spinal Cord Injury

To evaluate the effect of rapamycin treatment on locomotor recovery after SCI, Basso mouse scale (BMS) was measured for 6 weeks [30]. In our result, the rapamycin-treated mice had significantly higher BMS scores than the vehicle-treated mice from 3 to 6 weeks. This data supports the neuroprotection produced by mTOR inhibition can improve locomotor function after SCI.